analytical chemistry

Article

pubs.acs.org/ac

Multijunction Capillary Isoelectric Focusing Device Combined with Online Membrane-Assisted Buffer Exchanger Enables Isoelectric Point Fractionation of Intact Human Plasma Proteins for Biomarker Discovery

Mohammad Pirmoradian,[†,‡] Juan Astorga-Wells,[†,‡] and Roman A. Zubarev*[,†]

[†]Department of Medical Biochemistry and Biophysics, Karolinska Institutet, Scheeles väg 2, SE-17177 Stockholm, Sweden
[‡]Biomotif AB, SE-18212 Stockholm, Sweden

ABSTRACT: Prefractionation of proteins is often employed to improve analysis specificity in proteomics. Prefractionation based on the isoelectric point (pI) is particularly attractive because pI is a well-defined parameter and it is orthogonal to hydrophobicity on which reversed-phase chromatography is based. However, direct capillary electrophoresis of blood proteins is challenging due to its high content of salts and charged small molecules. Here, we couple an online desalinator device to our multijunction capillary isoelectric focusing (MJ-CIEF) instrument and perform direct isoelectric separation of human blood plasma. In a proof-of-principle experiment, pooled samples of patients with progressive mild cognitive impairment and corresponding healthy controls were investigated. Injection of 3 μL of plasma containing over 100 μg of proteins into the desalinator was followed by pI fractionation with MJ-CIEF in less than 1 h. Shotgun proteomics of 12 collected fractions from each of the 5 replicates of pooled samples resulted in the identification and accurate quantification (median CV between the replicates is <4%) of nearly 365 protein groups from 4030 unique peptides (with <1% FDR for both peptides and proteins). The obtained results include several proteins previously reported as AD markers. The isoelectric point of each quantified protein was calculated using a set of 7 synthetic peptides spiked into the samples. Several proteins with a significant pI shift between their isoforms in the patient and control samples were identified. The presented method is straightforward, robust, and scalable; therefore, it can be used in both biological and clinical applications.

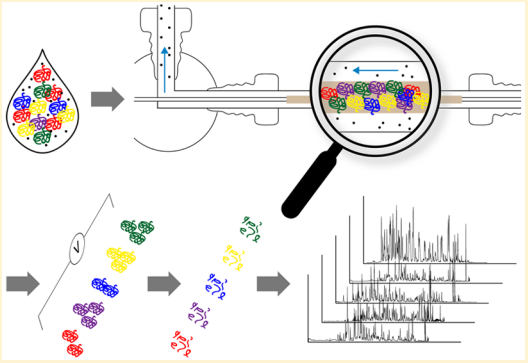

Blood plasma is a primary clinical specimen, and its analysis by mass spectrometry (MS) is of tremendous interest for biomarker discovery.[1] Besides blood-specific proteins, plasma also contains various proteins from both active secretion as well as cell and tissue leakage.[2] These proteins, which are typically found at extremely small concentrations, are potential biomarkers of different physiological and pathological states.[1] The large dynamic range of protein concentrations (over 11 orders of magnitude) is the greatest challenge for MS-based blood proteomics studies.[3] Consequently, research efforts are focused toward the development of a method for overcoming this difficulty, such as depletion of highly abundant proteins by immunoaffinity separation, which has become the dominant approach in blood plasma proteomics. Today, there are dozens of commercial kits and laboratory methods available for the removal of most of the highly abundant proteins through a single operation or serial depletion steps.[4−6] For instance, Qian et al. presented the tandem IgY12-SuperMix immunoaffinity system that removes ∼60 of the most abundant plasma proteins. Digestion of the remaining proteins followed by separation of tryptic peptides by off-line strong cation exchange (SCX) resulted in the identification of 695 proteins by LC-MS/MS analysis.[7] Jones et al. applied a similar method in an interlaboratory comparison of the performances of several high-resolution mass spectrometers. Two rounds of IgY14/Supermix immunoaffinity depletion in combination with iTRAQ 4-plex labeling followed by isoelectric focusing of labeled peptides and their separation into 30 fractions resulted in quantification of 1200−1700 proteins.[8] Recently, Keshishian et al. improved the whole protocol and succeeded in identifying 5300 proteins in 16 samples.[3] However, besides added complexity and cost, this method has other significant drawbacks, such as the unwanted removal of some nontargeted proteins and an increase in the overall variability of protein abundances.[9,10]

An alternative approach to protein depletion is the enrichment of target proteins or peptides from blood plasma. When the glycosylation pattern of proteins is of interest, glycosylated polypeptides can be enriched using lectin columns.[11,12] The enrichment strategy for tissue-leakage proteins is the isolation of plasma microparticles and exosomes.[13] Many cell types release into blood microparticles (large vesicles from 100 nm to 1 μm) and exosomes (smaller vesicles from 40 to 100 nm) and contain

Received: September 2, 2015
Accepted: November 3, 2015
Published: November 4, 2015

DOI: 10.1021/acs.analchem.5b03344
Anal. Chem. 2015, 87, 11840−11846

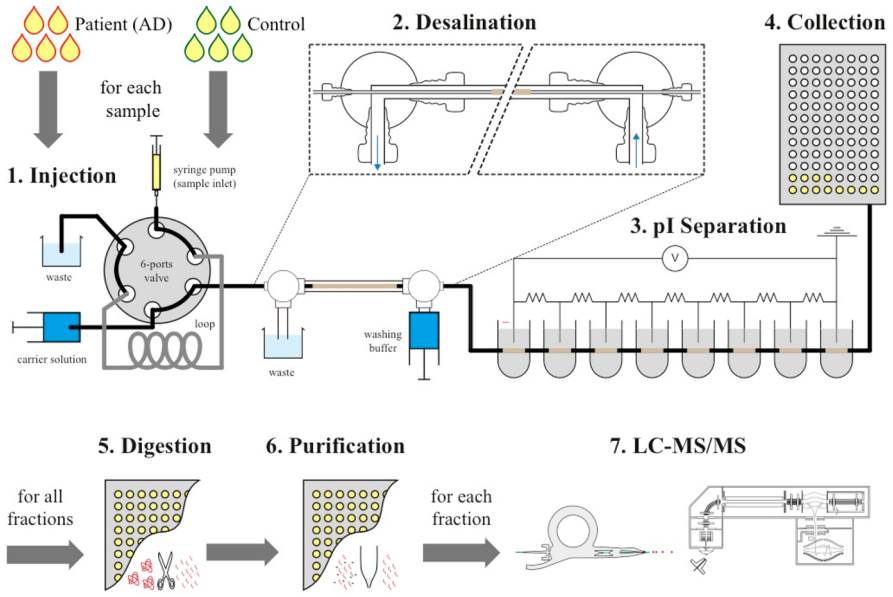

Figure 1. General workflow of blood plasma proteomic analysis using the combined desalinator-MJ-CIEF device. Raw blood plasma samples are injected via a 6-port valve (Step 1) and pass through the desalinator where buffer exchange occurs (Step 2). Then, the sample enters the pI separation column (Step 3) across which an electrical field is applied. After separation is completed, fractions are collected (Step 4) with each fraction being digested (Step 5) and purified (Step 6). Each fraction is then subjected to LC-MS/MS analysis (Step 7).

cell-specific proteins that represent potential biomarkers.[14] In a recent work, Harel et al. studied the microparticle proteome and developed the PROMIS-Quan method that expanded the plasma proteome to more than 3200 proteins.[2] However, because proteomics of tissue-leakage vesicles requires large sample amounts and precise storage and handling of the sample to avoid lysis of the microparticles before their isolation from plasma, the microparticle proteome remains much more challenging analytically than the core proteome of blood plasma.

Besides protein depletion or enrichment from blood plasma, many researchers increase the depth of proteomics analysis by employing prefractionation using conventional separation techniques, such as chromatography and electrophoresis. These methods are used either for proteins, as a first dimension of separation, or after digestion, when the resultant peptides are fractionated prior to LC-MS/MS analysis.[1] In a recent comparative study, Gautam et al. investigated three different approaches: abundant protein depletion followed by gel electrophoresis fractionation, depletion followed by fractionation of peptides by strong cationic exchange (SCX), and depletion only. They could identify 342 protein groups in the first approach, 251 protein groups in the second, and 194 protein groups from the depletion-only approach.[15] Therefore, prefractionation of plasma proteins clearly helps to increase the depth of analysis.

The advantage of using isoelectric focusing for prefractionation is not only in the reduction of sample complexity but also in grouping polypeptides by their isoelectric point (pI). pI is an informative parameter[16] that can be calculated rather precisely based on amino acid sequence.[17,18] To date, the wide use of isoelectric focusing for polypeptide prefractionation prior to LC-MS/MS analysis has been hampered by low throughput, as well as the time-consuming, labor-intensive, and costly nature of most commercial implementations of this technique. Recently, we introduced a multijunction capillary isoelectric focusing device (MJ-CIEF) that is free from these drawbacks and can be applied to both proteins and peptides.[19,20] The sample is injected into the MJ-CIEF in a small (1−3 μL) volume that can contain up to 100 μg of polypeptides. The separation step lasts for approximately an hour, and separated fractions can be directly injected into a reversed-phase column without additional clean-up or buffer exchange.

However, direct separation of blood plasma proteins by MJ-CIEF is precluded by the high salt concentration (136−145 mM of sodium), which determines the high electrical conductivity of the plasma, This, in turn, interferes with the electrophoresis of polypeptides. The use of off-line desalting cartridges or dialysis devices could help but would reduce MJ-CIEF's main advantages, such as the online character, ease of operation, speed of fractionation, and, last but not least, the very low sample losses.[19−21] To preserve these advantages, we added an online microdialysis desalinator to MJ-CIEF and integrated it with the overall MJ-CIEF workflow. Here, we demonstrate that the combined device enables direct and efficient separation of blood plasma proteins, and that the quality of protein fractionation by pI is sufficient for the use of this device in biomarker discovery. The performance of the combined device was tested on samples related to Alzheimer's disease (AD).

EXPERIMENTAL SECTION

Plasma Samples. Detailed descriptions of sample collection and preparation, clinical considerations, procedures, and ethical aspects are previously explained in detail elsewhere.[22] All 24 samples were from female donors with ages of 71 ± 3 years. Twelve samples of progressive mild cognitive impairment (PMCI) and an equal number of healthy controls were pooled into two respective samples. In addition, a standard blood plasma sample was purchased from Sigma-Aldrich, USA.

Desalinator Device. The overall setup is shown in Figure 1. The dialysis cell has a configuration previously reported for online hydrogen/deuterium exchange.[23] It consists of two coaxial tubes. The central tube, a 5-cm long tubular Nafion membrane with an inner diameter of 356 μm, passes through an FEP tube with a 2-mm inner diameter. The Nafion membrane is

DOI: 10.1021/acs.analchem.5b03344
Anal. Chem. 2015, 87, 11840−11846

connected to a capillary 1/32″ PEEK tube with one side attached to the sample injector and the other to the capillary isoelectric focusing column. The outer FEP tube is attached to two T-connectors with one end linked to the washing buffer pump and the other end to the waste collector. This configuration provides active microdialysis with a counter-flow of sample (inside the Nafion membrane) and washing buffer (inside the FEP tube) for maximizing the dialysis rate.

MJ-CIEF Device. A multiple-junction capillary was assembled as previously described in detail.[19,20] In brief, seven equal PEEK tubing segments (each 1.2 cm long, OD 635 μm, ID 395 μm) are connected together by interval tubular Nafion membranes (0.2-cm long, OD 610 μm, ID 330 μm). The assembly passes through eight serially connected Eppendorf vials (0.5 mL) that serve as containers for external electrolytic solutions. The front end of the MJ-CIEF is coupled with the desalinator device via 2-cm long PEEK tubing (OD 635 μm, ID 125 μm). A voltage divider built of seven serially connected 1 MΩ, 1 W resistors provides a linear voltage drop across the vials. The terminal contacts, as well as intermediate contacts between every two resistors, are connected to platinum wires inserted into the corresponding vials. The two terminal electrodes of the divider are attached to a DC power supplier (ARB 30 from Bertran, Hicksville, NY, USA).

Desalination and pI Separation of Plasma Proteins. Each pooled sample was fractionated and analyzed in five replicates. Each time, 3 μL of sample was loaded into a 3 μL loop connected to a 6-port injector valve (VICI Valco, USA) and transferred into the desalinator device by applying carrier buffer flow (5% of isopropanol and 1% of Pharmalyte 3-10 in milliQ distilled water) for 4 min at a flow rate of 1 μL/min. The loaded sample was buffer-exchanged with washing solution (same composition as carrier buffer) at 500 μL/min for 10 min. Thereafter, the sample was transferred into the capillary isoelectric focusing device for pI separation.

As in previous experiments, external electrolytic buffer solutions (acetic acid, ammonium acetate, ammonium formate, ammonium bicarbonate, and ammonia) were all prepared at 10 mM concentration in degassed Milli-Q water.[20] The buffers set the pH in each vial, thus creating a pH gradient across the whole device: from pH 3 in the anodic vial, to pH 4−9 in interval vials, and to pH 10 in the cathodic vial. Floating high voltage of up to −3 kV was applied to the cathodic vial, with the anodic vial being grounded, creating a field of 300 V/cm across the 10-cm long device in the regime of constant current of 40 μA. Isoelectric focusing was considered accomplished when the voltage increase subsided over time, which usually took less than 50 min. Focused fractions were then mobilized and collected at a flow rate of 0.5 μL/min with −0.2 kV applied to the cathode during mobilization. Three-time stepwise release and refocusing were applied during fraction elution as described in detail previously.[20] In each experiment, 12 fractions of 1 μL each were collected.

Protein Digestion. Proteins in each fraction were digested in solution by trypsin as described previously.[24] In brief, proteins were reduced with DTT (final concentration of 10 mM) for 20 min at 60 °C followed by alkylation via incubation with 10 mM iodoacetamide for 30 min at room temperature in the dark. Proteins were digested with trypsin (sequencing grade trypsin from Promega) incubated at 37 °C overnight. The digestion was terminated by the addition of 5% acetic acid (vol.) and rigorously vortexed over 5 min. All peptide mixtures were purified using Hypersep Filter Plate C-18 at 5−7 μL (Thermo Scientific) according to the manufacturer's protocol. Samples were dried using a SpeedVac and resuspended in water with 0.1% formic acid and 2% ACN.

RPLC-MS/MS Analysis. All fractions were analyzed in a random order using 70 min long RPLC-MS/MS analysis.[24] In brief, LC separation was performed with an EASY-Spray column (PepMap RSLC, C_{18} material with 100 Å pores, 3 μm-bead-packed 15-cm column) connected to an Easy-nLC 1000 pump (both from Thermo Scientific) with a 54 min gradient at a flow rate of 250 nL/min. The gradient went from 2 to 5% of buffer B (99.9% acetonitrile, 0.1% formic acid) in 6 min and then to 19% in 44 min and finally to 30% in 9 min. The gradient was followed by a 5 min washing step in 95% buffer B. Mass spectra were acquired with an Orbitrap Q Exactive Plus mass spectrometer (Thermo Fisher Scientific) in a data-dependent manner using a top-10 MS/MS method. Mass spectra were acquired at a resolution of 70,000 with a target value of 3×10^6 ions or a maximum accumulation time of 250 ms. The m/z range was from 300 to 2000. MS/MS spectra were acquired using HCD fragmentation with a normalized collision energy (NCE) of 25 at a resolution of 17,500 with a target value of 2×10^5 ions or a maximum accumulation time of 120 ms. The fixed isolation window for precursors was 3.0 Th, and the lowest m/z for fragments was 100.

Data Analysis. All raw data files were analyzed with MaxQuant, version 1.5.0.25, for peptide and protein identification and quantification.[25] The International Protein Index (human version 3.87) was used as a sequence database. The MS/MS search was performed with a 20 ppm mass tolerance for precursor ions in the initial search and a 6 ppm tolerance in the main search. Cysteine carbamidomethylation was selected as a fixed modification, and oxidation of methionine and N-acetylation of protein were selected as variable modifications. The matched peptides were allowed to contain up to two missed cleavages. The results were filtered to a 1% false discovery rate (FDR) at both protein and peptide levels[25] with proteins identified by peptides with a minimum length of 7 amino acids. Further data analysis was performed on the proteinGroups.txt file after removing potential contaminants as well as proteins that were identified in the reverse database. The MaxQuant-reported "LFQ-intensity" of each protein was taken as relative protein abundance.[26] These values were normalized by the median of all values in each sample and transformed by log2. Statistical tests and calculations were performed using Microsoft Excel and R. The focusing position for each protein was determined, as previously described,[20] as the centroid of the position calculated based on the MaxQuant-reported iBAQ-intensity values in individual fractions. Calculated focusing-position values in each sample were then normalized by the median of values in that sample.

RESULTS AND DISCUSSION

Desalinator Performance and Molecular Cutoff. Besides salts, blood plasma contains small molecules (e.g., amino acids, glycose, hormones, etc.) that may also interfere with electrophoresis. Therefore, it is important to remove these molecules before fractionation and yet not to lose proteins. Ideally, the cutoff level for the desalinator should be in the range of 300−500 Da, which is not only significantly below the size of the smallest protein (insulin, 5.8 kDa) but is also smaller than the mass of many neuropeptides.

To determine the molecular cutoff for our desalinator, we prepared a mixture of several amino acids and peptides over a wide range of molecular weights. In a series of experiments, this

DOI: 10.1021/acs.analchem.5b03344
Anal. Chem. 2015, 87, 11840−11846

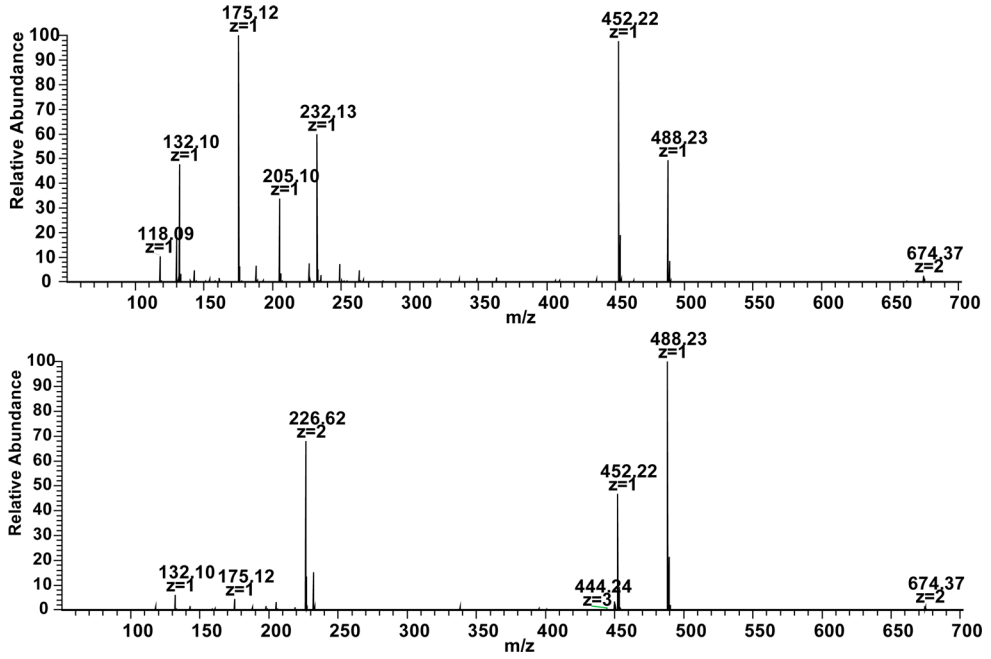

Figure 2. Mass spectra of a molecular mixture illustrating the mass cutoff of the desalinator at ∼400 Da (top) before and (bottom) after desalination. The mixture contains the amino acids L-leucine, L-valine, L-arginine, and L-tryptophan at m/z 118.09, 132.10, 175.12, and 205.10, respectively, as well as peptides GGYR, acetyl-SDKP, and RPKPQQFFGLM at m/z 452.22, 488.23, and 1348.64, respectively.

mixture was injected into the unit with or without washing with water for 10 min and then collected for mass analysis. Samples were injected into a mass spectrometer (Orbitrap XL) using a Nanomate autosampler (Advion). Comparison of the relative abundances of amino acids and peptides showed that molecules with molecular weights less than ∼400 Da are removed by washing (Figure 2). This molecular cutoff is sufficient to effectively remove both salts and small molecules from peptides and proteins of the injected sample.

Label-Free Quantification of Plasma Proteins. Analysis of all LC-MS/MS data sets resulted in the identification of 4030 unique peptides at an FDR of <1%. The matched peptides belong to 883 protein groups of which 365 groups passed the 1% FDR threshold. An additional 23 proteins had at least 2 peptides (at least 1 unique peptide) that covered more than 20% of the protein sequence.

In further analysis, only proteins that passed the 1% FDR criterion were used, which is a stricter approach than in many previously reported blood plasma proteome studies.

For comparison, unfractionated standard blood plasma was analyzed in ten replicates using the same LC-MS/MS setup. Significantly fewer numbers of unique peptides and protein groups were detected with <1% FDR (2571 and 206, respectively). This result confirms that the prime objective—an increase in the depth of blood plasma proteome analysis—was achieved.

The MaxQuant-reported LFQ intensities of protein groups were logarithmically transformed to reduce the effect of the large dynamic range of protein abundances and then normalized by subtraction of the median value in each sample. The median CV of the protein abundances between the replicates was 3.8%, which is a very low value by the standards of proteomics analyses applied to biomarker discovery.[27,28] A median value of $R = 0.961$ was obtained for Pearson correlations between all replicates, indicating high reproducibility of the method (Figure 3).

To assess the utility of the fractionated proteome for biomarker discovery, the normalized protein abundances were compared between the pooled patient and control samples (Figure 4). The top ten proteins with an abundance difference of over 10% and a p-value of less than 0.05 (based on Student's t test) were selected for detailed investigation. Several of these proteins have previously been reported as exhibiting an abundance difference in AD, e.g., alpha-2-macroglobulin,[29,30] plasminogen,[31] as well as members of the complement system[32] and serpin family.[33,34] The directions of the abundance changes in our study coincide with those reported in literature.

There is extensive knowledge implicating the proteins mentioned above in AD-related processes. The presence of proteinase inhibitor alpha-2-macroglobulin (A2M) was shown in amyloid plaques.[35] It is also a potential marker of damage to the blood-brain barrier.[36] Upregulation of this molecule was reported to be induced by cytokines, implicating it in regulation of the immune response.[37,38] Plasmin was shown to promote Aβ peptide clearance.[39] Conversely, Aβ plays a modulatory role for the tissue plasminogen activator (tPA)/plasmin system by enhancing the proteolytic activity of tPA.[40] Activation of contact system and fibrinolysis results in the generation of peptides like kallikerin and plasmin, which can consequently activate the classical pathway of the complement system in a C1q-independent manner.[41] The possibility of a stimulatory effect of soluble Aβ peptides in the activation of these systems in the AD brain was suggested by in vivo findings.[42,43] Therefore, the fact that the abundances of these proteins changed in our study is strongly supported by the literature.

Focusing Position of Blood Plasma Proteins. For 146 quantified proteins, it was possible to calculate their focusing position in at least three of the five replicates. The calculation was based on the centroid of a peak composed by the abundances of these proteins in adjacent pI fractions. Previously, this method has been implemented by us for peptides.[20] The median CV between the replicates of the thus-determined positions was

DOI: 10.1021/acs.analchem.5b03344
Anal. Chem. 2015, 87, 11840−11846

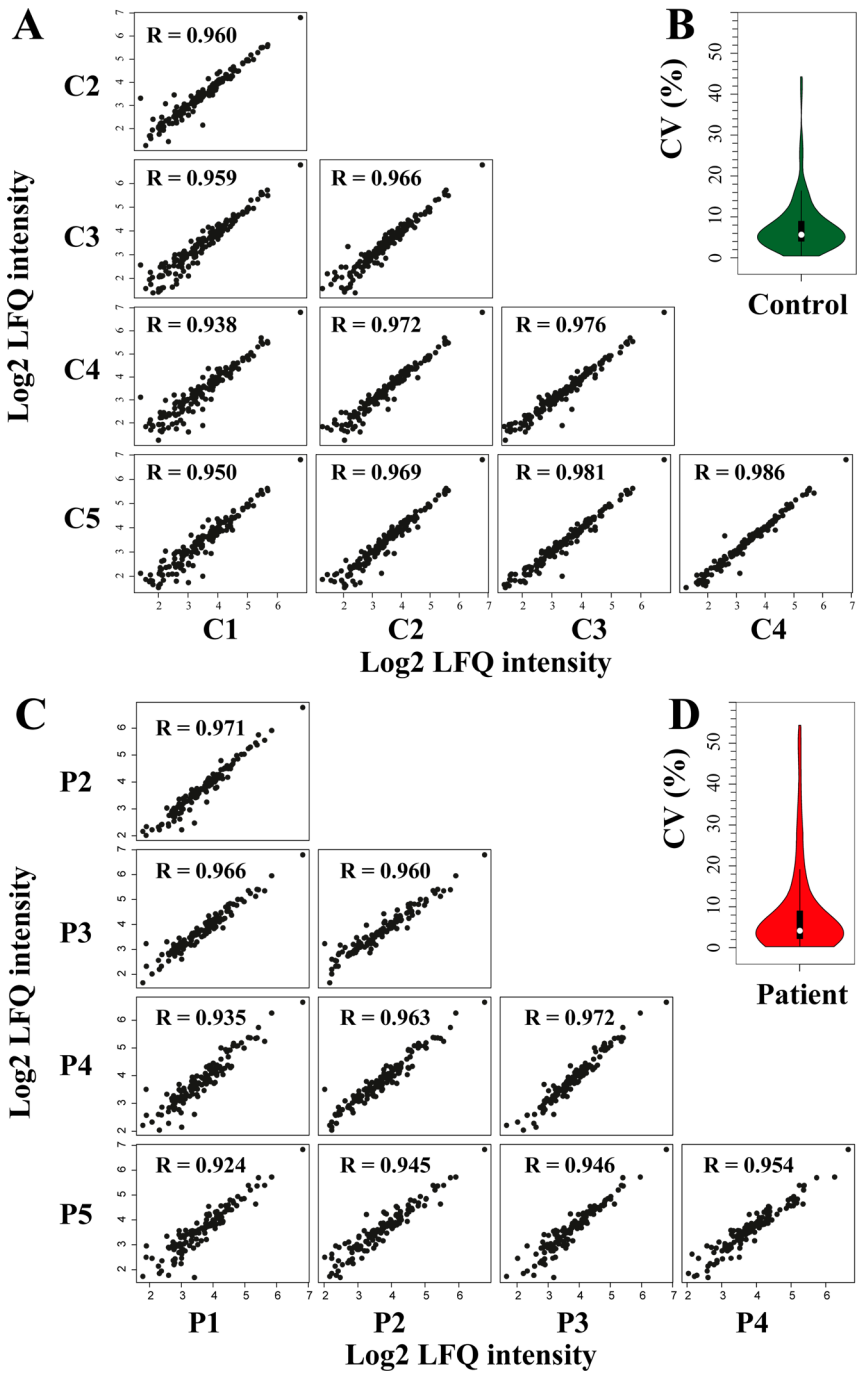

Figure 3. Correlation between the log2 transformed protein abundances in replicate fractionation experiments and the CV distribution of protein abundances: (A, B) healthy samples and (C, D) patient samples. Each dot represents one protein.

3.5%, indicating that this parameter can be measured experimentally with a rather high accuracy. For each protein, the positional difference between the patient and control samples was then calculated with its statistical significance evaluated by the *p*-value (Figure 5). Proteins with significant positional differences ($p = 0.05$ threshold used) are listed in Table 1. The detected pI differences were always negative for proteins in Table 1, suggesting a shift to more acidic values in samples from PMCI patients. These differences could be due either to post-translational modifications (PTMs) or truncations. Among the PTMs inducing acidic pI shift are phosphorylation and deamidation. We reanalyzed by Max Quant the fractions corresponding to the central positions of kinesin-like protein, thyroxine-binding globulin, and Msx2-interacting protein using phosphorylation of Ser, Thr, and Tyr and deamidation of Asn and Gln as flexible modifications. Although both kinesin-like protein and thyroxine-binding globulin have known sites of phosphorylation, we did not detect peptides with this PTM. Therefore, either the phosphorylation occurred on undetected peptides of these proteins, or the pI difference was due other modifications and/or truncations. In contrast, several sites of Asn deamidations for Msx2-interacting protein were identified in samples from patients with PMCI. Because Asn deamidation leads to the formation of damaging isoaspartyl (isoAsp) residues, this finding supports the earlier results that linked elevated isoAsp levels in blood plasma with AD progression.[44] Therefore,

DOI: 10.1021/acs.analchem.5b03344
Anal. Chem. 2015, 87, 11840−11846

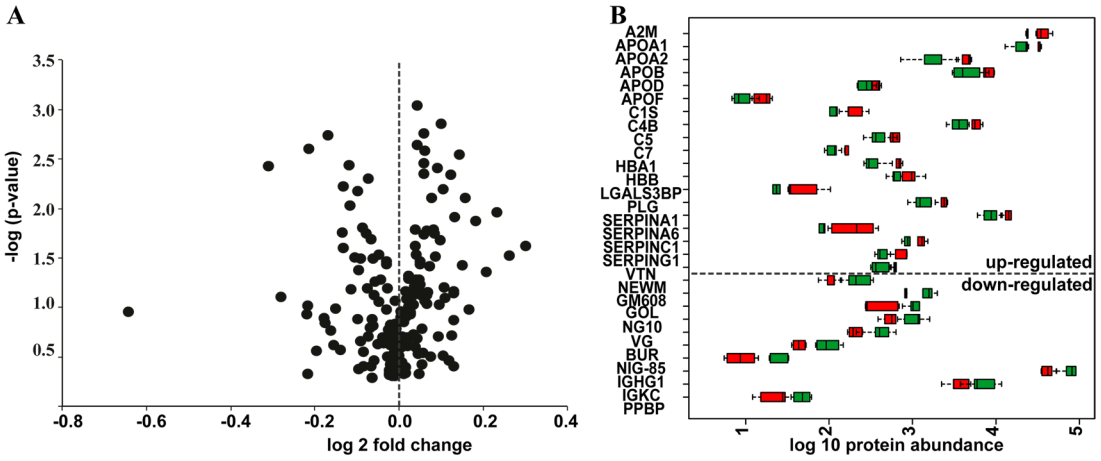

Figure 4. (A) A volcano plot of the protein abundance ratios in healthy vs patient samples. The *x*-axis is the log2 of the ratio between the median abundances of a protein in patient samples and healthy samples. The *y*-axis is the −log10 of *p*-values associated with each ratio. Each dot represents one protein. (B) Box plot of the most significantly changed protein abundances in healthy (green) and patient (red) samples.

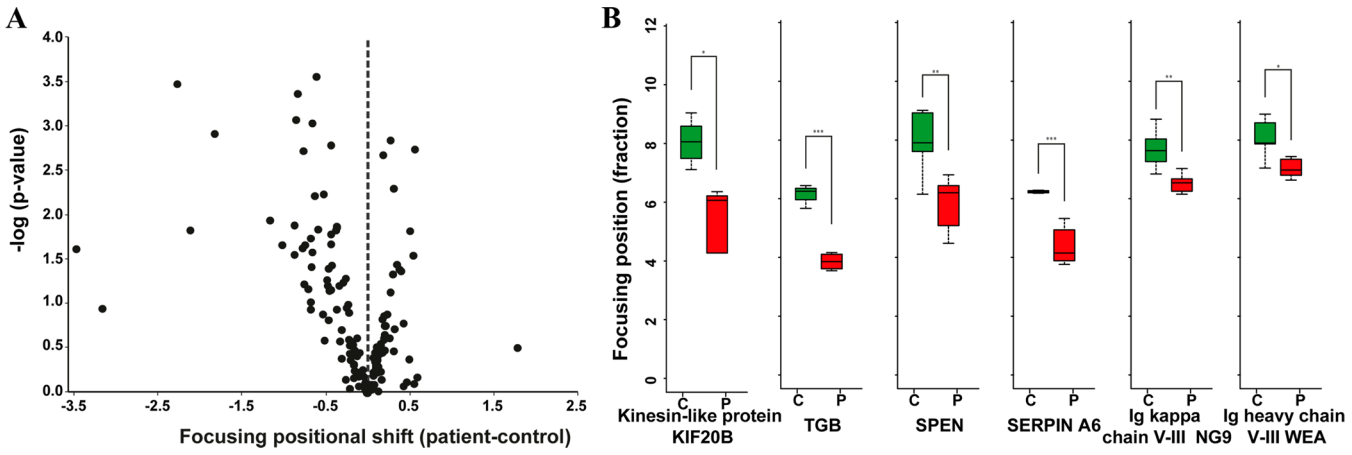

Figure 5. (A) A volcano plot of the focusing positions. The *x*-axis is the difference between the median of central focusing positions of a protein in patient samples and healthy samples. The *y*-axis is the −log10 of the *p*-value associated with the positional shift. Each dot represents one protein. (B) Box plot of significantly changed focusing positions of proteins in healthy (green) and patient (red) samples.

Table 1. Proteins with Significant Difference in Their Central Focusing Position between Healthy and Patient Samples with a Negative Shift Meaning More Acidic Protein

protein	positional shift, arb. units	*p*-value
Kinesin-like protein KIF20B	−3.5	0.0122
Thyroxine-binding globulin	−2.3	0.0001
Msx2-interacting protein	−2.1	0.0072
Corticosteroid-binding globulin	−1.8	0.0005
Ig kappa chain V−III region NG9	−1.2	0.0056
Ig heavy chain V−III region WEA	−1.0	0.0105
Ig kappa chain V−II region TEW	−0.9	0.0063
Alpha-1-antitrypsin	−0.9	0.0135

pI shift can be used as a complementary parameter for detecting deamidation products.

CONCLUSIONS

Here, we developed an online desalinator device and coupled it with the earlier developed capillary isoelectric focusing fractionator, applying this novel combination for direct pI-based separation of proteins in blood plasma. Solution fractionation has clear advantages over gel-based separation with respect to speed, convenience, and reduction of losses; these advantages were preserved in the combined device. As a proof of principle, analysis of blood plasma samples from patients with progressive Alzheimer's disease versus age-matched healthy individuals confirmed that the prime objective of the current work—to increase the depth of blood plasma proteome analysis—was achieved. Importantly, the proteomics analysis retained its high reproducibility, as witnessed by the low CV values and high correlation between the replicates.

Besides the increased depth of analysis, the fractionating device offers an additional advantage, which is to measure the pI shift of a given protein in patient samples. Such measurements can provide another domain for biomarker discovery. This additional dimension may be important for diseases involving protein modification, including truncation. Indeed, in AD, where elevated isoAsp levels in blood are linked to the risk of developing dementia,[44] an increased level of deamidation in blood proteins may be a potential biomarker for that risk. Furthermore, because deamidation involves a negative shift in pI, the change in average deamidation status should be easily detectable. In our next work, we plan to use these new opportunities offered by the combined device and investigate in detail the proteins undergoing pI shift in AD.

DOI: 10.1021/acs.analchem.5b03344
Anal. Chem. 2015, 87, 11840−11846

In summary, the addition of an online desalinator made the MJ-CIEF device suitable for direct proteomics analysis of blood plasma in a fast, reproducible, and low-cost manner, offering analytical advantages for both global proteomics as well as targeted protein(s) analyses.

AUTHOR INFORMATION

Corresponding Author

*E-mail: roman.zubarev@ki.se. Phone: +46 8 524 87594.

Notes

The authors declare no competing financial interest.

ACKNOWLEDGMENTS

This work was supported by the Swedish Research council (Grant 2011-3699), Alzheimersfonden, VINNOVA Foundation (grant within the EuroStar 2010 Programme), and the Knut and Alice Wallenberg Foundation (Grant KAW 2010.0022).

REFERENCES

(1) Pernemalm, M.; Lehtio, J. *Expert Rev. Proteomics* **2014**, *11*, 431−48.
(2) Harel, M.; Oren-Giladi, P.; Kaidar-Person, O.; Shaked, Y.; Geiger, T. *Mol. Cell. Proteomics* **2015**, *14*, 1127−36.
(3) Keshishian, H.; Burgess, M. W.; Gillette, M. A.; Mertins, P.; Clauser, K. R.; Mani, D. R.; Kuhn, E. W.; Farrell, L. A.; Gerszten, R. E.; Carr, S. A. *Mol. Cell. Proteomics* **2015**, *14*, 2375.
(4) Shuford, C. M.; Hawkridge, A. M.; Burnett, J. C., Jr.; Muddiman, D. C. *Anal. Chem.* **2010**, *82*, 10179−85.
(5) Tan, S. H.; Mohamedali, A.; Kapur, A.; Baker, M. S. *J. Proteome Res.* **2013**, *12*, 2399−413.
(6) Shi, T.; Zhou, J. Y.; Gritsenko, M. A.; Hossain, M.; Camp, D. G., 2nd; Smith, R. D.; Qian, W. J. *Methods* **2012**, *56*, 246−53.
(7) Qian, W. J.; Kaleta, D. T.; Petritis, B. O.; Jiang, H.; Liu, T.; Zhang, X.; Mottaz, H. M.; Varnum, S. M.; Camp, D. G., 2nd; Huang, L.; Fang, X.; Zhang, W. W.; Smith, R. D. *Mol. Cell. Proteomics* **2008**, *7*, 1963−73.
(8) Jones, K. A.; Kim, P. D.; Patel, B. B.; Kelsen, S. G.; Braverman, A.; Swinton, D. J.; Gafken, P. R.; Jones, L. A.; Lane, W. S.; Neveu, J. M.; Leung, H. C.; Shaffer, S. A.; Leszyk, J. D.; Stanley, B. A.; Fox, T. E.; Stanley, A.; Hall, M. J.; Hampel, H.; South, C. D.; de la Chapelle, A.; Burt, R. W.; Jones, D. A.; Kopelovich, L.; Yeung, A. T. *J. Proteome Res.* **2013**, *12*, 4351−65.
(9) Tu, C.; Rudnick, P. A.; Martinez, M. Y.; Cheek, K. L.; Stein, S. E.; Slebos, R. J.; Liebler, D. C. *J. Proteome Res.* **2010**, *9*, 4982−91.
(10) Bellei, E.; Bergamini, S.; Monari, E.; Fantoni, L. I.; Cuoghi, A.; Ozben, T.; Tomasi, A. *Amino Acids* **2011**, *40*, 145−56.
(11) Zielinska, D. F.; Gnad, F.; Wisniewski, J. R.; Mann, M. *Cell* **2010**, *141*, 897−907.
(12) Boersema, P. J.; Geiger, T.; Wisniewski, J. R.; Mann, M. *Mol. Cell. Proteomics* **2013**, *12*, 158−71.
(13) Jin, M.; Drwal, G.; Bourgeois, T.; Saltz, J.; Wu, H. M. *Proteomics* **2005**, *5*, 1940−52.
(14) Ostergaard, O.; Nielsen, C. T.; Iversen, L. V.; Jacobsen, S.; Tanassi, J. T.; Heegaard, N. H. *J. Proteome Res.* **2012**, *11*, 2154−63.
(15) Gautam, P.; Nair, S. C.; Ramamoorthy, K.; Swamy, C. V.; Nagaraj, R. *PLoS One* **2013**, *8*, e72584.
(16) Righetti, P. G.; Sebastiano, R.; Citterio, A. *Proteomics* **2013**, *13*, 325−340.
(17) Sillero, A.; Maldonado, A. *Comput. Biol. Med.* **2006**, *36*, 157−166.
(18) Halligan, B. D.; Ruotti, V.; Jin, W.; Laffoon, S.; Twigger, S. N.; Dratz, E. A. *Nucleic Acids Res.* **2004**, *32*, W638−W644.
(19) Chingin, K.; Astorga-Wells, J.; Pirmoradian Najafabadi, M.; Lavold, T.; Zubarev, R. A. *Anal. Chem.* **2012**, *84*, 6856−62.
(20) Pirmoradian, M.; Zhang, B.; Chingin, K.; Astorga-Wells, J.; Zubarev, R. A. *Anal. Chem.* **2014**, *86*, 5728−32.
(21) Kim, K. H.; Compton, P. D.; Tran, J. C.; Kelleher, N. L. *J. Proteome Res.* **2015**, *14*, 2199−206.
(22) Julkunen, V.; Niskanen, E.; Koikkalainen, J.; Herukka, S. K.; Pihlajamaki, M.; Hallikainen, M.; Kivipelto, M.; Muehlboeck, S.; Evans, A. C.; Vanninen, R.; Hilkka, S. *J. Alzheimer's Dis.* **2010**, *21*, 1141−51.
(23) Astorga-Wells, J.; Landreh, M.; Johansson, J.; Bergman, T.; Jornvall, H. *Mol. Cell. Proteomics* **2011**, *10*, M110.006510.
(24) Pirmoradian, M.; Budamgunta, H.; Chingin, K.; Zhang, B.; Astorga-Wells, J.; Zubarev, R. A. *Mol. Cell. Proteomics* **2013**, *12*, 3330−8.
(25) Cox, J.; Mann, M. *Nat. Biotechnol.* **2008**, *26*, 1367−72.
(26) Cox, J.; Hein, M. Y.; Luber, C. A.; Paron, I.; Nagaraj, N.; Mann, M. *Mol. Cell. Proteomics* **2014**, *13*, 2513−26.
(27) Anderson, N. L.; Anderson, N. G. *Mol. Cell. Proteomics* **2002**, *1*, 845−67.
(28) Mack, S.; Cruzado-Park, I.; Chapman, J.; Ratnayake, C.; Vigh, G. *Electrophoresis* **2009**, *30*, 4049−58.
(29) Hye, A.; Lynham, S.; Thambisetty, M.; Causevic, M.; Campbell, J.; Byers, H. L.; Hooper, C.; Rijsdijk, F.; Tabrizi, S. J.; Banner, S.; Shaw, C. E.; Foy, C.; Poppe, M.; Archer, N.; Hamilton, G.; Powell, J.; Brown, R. G.; Sham, P.; Ward, M.; Lovestone, S. *Brain* **2006**, *129*, 3042−50.
(30) Yang, H.; Lyutvinskiy, Y.; Herukka, S. K.; Soininen, H.; Rutishauser, D.; Zubarev, R. A. *J. Alzheimer's Dis.* **2014**, *40*, 659−66.
(31) Oh, J.; Lee, H. J.; Song, J. H.; Park, S. I.; Kim, H. *Exp. Gerontol.* **2014**, *60*, 87−91.
(32) Bergamaschini, L.; Canziani, S.; Bottasso, B.; Cugno, M.; Braidotti, P.; Agostoni, A. *Clin. Exp. Immunol.* **1999**, *115*, 526−33.
(33) Liao, P. C.; Yu, L.; Kuo, C. C.; Lin, C.; Kuo, Y. M. *Proteomics: Clin. Appl.* **2007**, *1*, 506−12.
(34) Doecke, J. D.; Laws, S. M.; Faux, N. G.; Wilson, W.; Burnham, S. C.; Lam, C. P.; Mondal, A.; Bedo, J.; Bush, A. I.; Brown, B.; De Ruyck, K.; Ellis, K. A.; Fowler, C.; Gupta, V. B.; Head, R.; Macaulay, S. L.; Pertile, K.; Rowe, C. C.; Rembach, A.; Rodrigues, M.; Rumble, R.; Szoeke, C.; Taddei, K.; Taddei, T.; Trounson, B.; Ames, D.; Masters, C. L.; Martins, R. N.; Alzheimer's Disease Neuroimaging, I.; Australian Imaging, B.; Lifestyle Research, G.. *AMA Arch. Neurol.* **2012**, *69*, 1318−25.
(35) Bauer, J.; Strauss, S.; Schreiter-Gasser, U.; Ganter, U.; Schlegel, P.; Witt, I.; Yolk, B.; Berger, M. *FEBS Lett.* **1991**, *285*, 111−4.
(36) Cucullo, L.; Marchi, N.; Marroni, M.; Fazio, V.; Namura, S.; Janigro, D. *Mol. Cell. Proteomics* **2003**, *2*, 234−41.
(37) Strauss, S.; Bauer, J.; Ganter, U.; Jonas, U.; Berger, M.; Volk, B. *Lab. Invest.* **1992**, *66*, 223−30.
(38) Armstrong, P. B.; Quigley, J. P. *Advances in experimental medicine and biology* **2001**, *484*, 141−60.
(39) Tucker, H. M.; Kihiko-Ehmann, M.; Wright, S.; Rydel, R. E.; Estus, S. *J. Neurochem.* **2000**, *75*, 2172−7.
(40) Kingston, I. B.; Castro, M. J.; Anderson, S. *Nat. Med.* **1995**, *1*, 138−42.
(41) Kaplan, A. P.; Joseph, K.; Shibayama, Y.; Reddigari, S.; Ghebrehiwet, B.; Silverberg, M. *Adv. Immunol.* **1997**, *66*, 225−72.
(42) Yasuhara, O.; Walker, D. G.; McGeer, P. L. *Brain Res.* **1994**, *654*, 234−40.
(43) Bergamaschini, L.; Parnetti, L.; Pareyson, D.; Canziani, S.; Cugno, M.; Agostoni, A. *Alzheimer Dis. Assoc. Disord.* **1998**, *12*, 102−8.
(44) Yang, H.; Lyutvinskiy, Y.; Soininen, H.; Zubarev, R. A. *J. Alzheimer's Dis.* **2011**, *27*, 113−8.

DOI: 10.1021/acs.analchem.5b03344
Anal. Chem. 2015, 87, 11840−11846